Catalytic cracking of n-Dodecane and Alkyl benzenes over FCC Zeolite Catalysts: Time on Stream and Reactant Converted Models

Nasir M. Tukur and Sulaiman Al-Khattaf[1]

Chemical Engineering Department

King Fahd University of Petroleum & Minerals

Dhahran 31261, Saudi Arabia

ABSTRACT

Catalytic cracking of three hydrocarbon model compounds (n-dodecane, 1,3,5-triisopropylbenzene, and 1,4-diisopropylbenzene) has been investigated over two FCC zeolite catalysts in a novel riser simulator that resembles closely the operating conditions of large scale FCC units. The catalytic cracking experiments were carried out at different reaction times and temperatures using the two FCC zeolite catalysts, FCC-B based on USY zeolite and FCC-GKF based on ZSM-5. The experimental results were modeled using quasi-steady state approximation with the catalyst activity decay function based on both time on stream (TOS) and reactant conversion model (RC). The kinetics for the n-dodecane cracking as well as for the two alkyl benzenes has been modeled as a first order process. The higher apparent activation energies of cracking observed over the USY-based catalyst (FCC-B) for n-dodecane, coupled with the lowest value observed for the same molecule over the ZSM-5 based catalyst (FCC-GKF), seems to suggest that stronger acid sites are more important for n-dodecane cracking as compared to alkyl benzenes where weaker acids are sufficient for dealkylation.

November 2004 (Revised)

Keywords: FCC, 1,3,5-triisopropylbenzene (1,3,5-TIPB), 1,4-diisopropylbenzene (1,4-DIPB), n-Dodecane, time on stream (TOS)

[1] To whom correspondence should be addressed, email skhattaf@kfupm.edu.sa

1. INTRODUCTION

Fluid Catalytic Cracking (FCC) process is one of the most important processes for gasoline production. FCC process has the basic objective of processing different feeds so as to increase the value of the resulting products. The first step in fluid catalytic cracking is the formation of carbenium ions. And once the ions are formed, different reactions proceed which include β-scission, isomerization, dealkylation, trans-alkylation, disproportionation, hydrogen transfer, among others.

Commercial FCC catalysts are based on Y zeolites as main component with ZSM-5 as additive. These zeolites are bounded individually in a spray dried matrix such as silica-alumina. It is reported that adding ZSM-5 additives promotes higher ratio of cracking to hydrogen transfer reactions than Y zeolite-based catalyst [1]. Furthermore, adding ZSM-5 to a catalytic cracker has little effect on the heavier components such as aromatic compounds. This can be due to the smaller ZSM-5 pore diameter (in the range of 5-6 Å) that restricts alkyl benzenes but allows normal paraffins and olefins to penetrate and react.

In order for hydrocarbon reactions to proceed in FCC catalysts, molecules have to first of all diffuse through the large matrix pores (500-5000 Å, composed of amorphous silica alumina), and then into the zeolite crystal. As a result, only certain molecules with certain molecular critical diameter can penetrate these zeolite structures. For example, Y-zeolite crystal is expected to host larger molecules than ZSM-5 crystals [2]. Those molecules which are larger than the maximum size that the crystal can allow to enter have to react either in the matrix if the matrix is active or on the external surface area of zeolite. This surface area represents only 3 % from the total surface area [3].

Due to its very large pore size, diffusion in the FCC matrix belongs to the Knudsen regime, while hydrocarbon diffusion in zeolites falls in the configurational regime [4, 5]. High diffusion activation energy is the most important characteristic of this regime [4]. In many cases, this activation energy is much higher than the reaction activation energy [2]. Hence it can be expected that in FCC catalyst system, zeolite crystal likely controls the reaction pathway.

The catalytic cracking of isopropyl benzene takes place through the cleavage of the propyl group from the benzene ring with the benzene ring remaining unchanged. 1,3,5-tri-isopropylbenzene (1,3,5-TIPB) has been used to study the relation between zeolite pore size and reaction pathway. Recently, Al-Khattaf et al., [5] have used this molecule to investigate the role of diffusion limitation in Y-zeolite. They concluded that due the high activation energy for 1,3,5-TIPB diffusion in Y-zeolite crystal at low reaction temperature, the reaction is controlled by diffusion. While it is reaction controlled at high temperature. Furthermore, Al-Khattaf and de Lasa [2] have cracked cumene, 1,3 di-isopropylbenzene and 1,3,5-TIPB by two different Y-zeolite crystal sizes. They reported the same conversion level at all reaction temperatures for cumene and 1,3 DIPB cracking using the two crystal sizes. However, in the case of 1,3,5-TIPB, the zeolite with small crystal shows higher conversion than the large crystal at low to medium reaction temperatures.

An interesting study was carried by Roos et al., [6] that used two different zeolites, MCM-41 and H-Y zeolite and Commercial FCC catalysts to crack 1,3,5-TIPB and C_{16}. It was found that accessibility to the internal acid sites affects both catalyst activity and selectivity, with MCM-41 zeolite yielding the higher 1,3,5-TIPB conversion. Regarding 1,3,5-TIPB reactivity over ZSM-5, it was clearly concluded that 1,3,5 TIPB can not penetrate ZSM-5 pores and thus has to react on the external ZSM-5 sites.

Paraffins, both linear and branched, comprised a significant proportion of many FCC feeds. There is ample evidence to support the fact that cracking of linear paraffins on HZSM-5 is initiated at Brønsted sites, through the initial formation of carbenium ion. And also a number of investigations have reached the conclusion that there is a direct correlation between cracking activity of n-paraffins on HZSM-5 and the number of Brønsted sites. [12] Corma et al., [13] studied the kinetics for the catalytic cracking of paraffins at very short times on streams (below 10s), and concluded that the influence of the adsorption terms in the kinetic expression is negligible, They further added that the catalyst decay is better represented by conversion-dependent time on stream function.

The use of ZSM-5 in FCC plants as an additive has also become very important in increasing both octane number and C_3-C_4 olefins. It is therefore of industrial significance to try to understand the cracking behavior of this zeolite as compared to Y zeolite with representative model compounds at different reaction conditions.

In the present study, a systematic investigation of catalytic cracking of two aromatic compounds (1,3,5-TIPB and 1,4-DIPB) and an alkane (n-dodecane) over two different catalysts (one based on Y zeolite and the second based on ZSM-5) will be carried out at different reaction times and temperatures. It is also the goal of the present study to evaluate the kinetic parameters of the cracking reactions based on both the "Time on Stream" and the "Reactant Converted" models.

2. EXPERIMENTAL PROCEDURE

2.1 The Riser Simulator

All the experimental runs were carried out in the riser simulator. This reactor is novel bench scale equipment with internal recycle unit invented by de Lasa [9] to overcome the technical problems of the standard micro-activity test (MAT). For example, the low olefinity obtained from MAT reactor, due to its higher reaction time (> 75 s) as compared to the riser (< 15 s), non uniform coke deposition (150 mm long catalyst bed), and temperature/concentration gradient, which have all been eliminated by the well-mixed characteristics and intense fluidization of the riser simulator. The riser simulator is fast becoming a valuable experimental tool for reaction evaluation involving model compounds [2, 5] and also for testing and developing new fluidized catalytic cracking in vacuum gas oil cracking [10, 11].

The riser simulator consists of two outer shells, the lower section and the upper section, which allow one to load or to unload the catalyst easily, as illustrated in Fig. 1. The reactor was designed in such a way that an annular space is created between the outer portion of the basket and the inner part of the reactor shell. A metallic gasket seals the two chambers with an impeller located in the upper section. A packing gland assembly and a cooling jacket surrounding the shaft provide support for the impeller. Upon rotation of the shaft, gas is forced outward from the center of the impeller toward the walls. This creates a lower pressure in the center region of the impeller, thus inducing flow of gas upward through the catalyst chamber from the bottom of the reactor annular region where the pressure is slightly higher. The impeller provides a fluidized bed of catalyst particles as well as intense gas mixing inside the reactor. A detailed description of various riser

simulator components, sequence of injection and sampling can be found in work by Kraemer [12].

2.2 Materials

Commercial Y- zeolite having a Si/Al atomic ratio of 2.6 provided by Tosoh Co. Japan was used in this work. The Na zeolite was ion exchanged with NH_4NO_3 to replace the Na cation with NH_4^+. Following this, NH_3 was removed and the H form of the zeolite was spray-dried using kaolin as the filler and a silica sol as the binder, both materials are supplied by Catalysts and Chemicals Industries Co. Japan. The resulting 60 μm catalyst particles had the following composition: 30 wt % zeolite, 50 wt % kaolin, and 20 wt % silica. The process of Na removal was repeated for the pelletized catalyst. Following this, the catalyst was calcined at 600^{o}C for 2 h. Finally, the fluidizable catalyst particles (60 μm average size) were treated with 100 % steam at 760^{o}C for 5 hours to obtain the dealuminated Y (designated USY) zeolites. Table 1 reports the catalyst main properties following catalyst pretreatment.

The ZSM-5 zeolite used in this work was ion exchanged with NH_4NO_3 to replace the Na cation with NH_4^+. Following this, NH_3 was removed and the H form of the zeolite was spray-dried using kaolin as the filler and a silica sol as the binder. The resulting 60 μm catalyst particles had the following composition: 30 wt % zeolite, 50 wt% kaolin, and 20 wt % silica. The process of Na removal was repeated for the pelletized catalyst. Following this, the catalyst was calcined at 600^{o}C for 2 h.

2.3 Catalyst characterization

The BET surface area was measured according to the standard procedure ASTM D-3663 using Sorptomatic 1800 Carlo Erba Strumentazione unit, Italy. The acid property of the catalyst was characterized by NH_3 temperature-programmed desorption (NH_3-TPD). In all the experiments, 50 mg of sample was outgassed at 400^{o}C for 30 min in flowing He and then cooled down to 150^{o}C. At that temperature, NH_3 was adsorbed on the sample by injecting pulses of 2 μl/pulse. The injection was repeated until the amount of NH_3 detected was the same for the last two injections. After the adsorption of NH_3 was

saturated, the sample was flushed at 150^{o}C for 1 h with He to remove excess NH_3, and then the temperature was programmed at 30 ^{o}C/min up to 1000^{o}C in flowing helium at 30 ml/min. Flame ionization detector was used to monitor the desorbed NH_3. Figure 2 shows the X-ray diffraction for both the two catalysts.

2.4. Procedure

Regarding the experimental procedure in the riser simulator, a 0.81 g portion of the catalyst was weighed and loaded into the riser simulator basket. The system was then sealed and tested for any pressure leaks by monitoring the pressure changes in the system. Furthermore, the reactor was heated to the desired reaction temperature. The vacuum box was also heated to around 250^{o}C and evacuated at around 0.5 psi to prevent any condensation of hydrocarbons inside the box. The heating of the riser simulator was conducted under continuous flow of inert gas (Ar), and it usually takes a few hours until thermal equilibrium is finally attained. Meanwhile, before the initial experimental run, the catalyst was activated for 15 min at 620^{o}C in a stream of Ar. The temperature controller was set to the desired reaction temperature, and in the same manner, the timer was adjusted to the desired reaction time. At this point the GC is started and set to the desired conditions.

Once the reactor and the gas chromatograph have reached the desired operating conditions, the feedstock was injected directly into the reactor via a loaded syringe. After the reaction, the four-port valve immediately opens, ensuring that the reaction was terminated and the entire product stream sent online to the analytical equipment via a preheated vacuum box chamber.

2.5 Analysis

The riser simulator operates in conjunction with a series of sampling valves that allow, following a predetermined sequence, one to inject reactants and withdraw products in short periods of time. The products were analyzed in an Agilent 6890N gas

chromatograph with a flame ionization detector and a capillary column INNOWAX, 60-m cross-linked methyl silicone with an internal diameter of 0.32 mm.

Experiments were carried out at different temperatures with constant catalyst/reactant ratio of 5 (weight of catalyst = 0.81g, weight of reactant injected = 0.162g). Typical errors in the conversion were in the ± 2%.

3. KINETIC MODELING

Wojciechowski and Corma [13] pointed out that FCC cracking of model compounds (such as cumene) follows a first order model. Reactant disappearance in a Riser Simulator has been represented effectively by the following equation assuming that the effectiveness factor is unity [14]:

$$\frac{-V}{W_c}\frac{dC_A}{dt} = k\,\varphi\,C_A \qquad (1)$$

where;

C_A= Reactant concentration in the Riser Simulator (mole/m^3)

V = volume of the riser (45 cm^3)

W_c = mass of the catalysts (0.81 gcat)

t = time (sec).

φ= deactivation function

k = rate constant (cm^3/gcat.sec).

The reactant concentration C_A can be expressed by the following relationship;

$$C_A = \frac{y_A W_{hc}}{MW_A V} \qquad (2)$$

where ;

y_A= reactant mass fraction (wt%)

W_{hc}= total mass inside the riser (0.162 g)

MW_A= molecular weight

Furthermore, k can be expressed by an Arrhenius equation:

$$k = k_o^{'} \exp\left(\frac{-E_R}{RT}\right) \tag{3}$$

Then eq. (1) can be re-written as:

$$\frac{-V}{W_c}\frac{dy_A}{dt} = k'_0 \exp\left(\frac{-E_R}{RT}\right)\varphi\, y_A \tag{4}$$

Introducing scaling, eq. (4) becomes:

$$\frac{-V}{W_c}\frac{dy_A}{dt} = k'_0 \exp\left[\frac{-E_R}{R}\left(\frac{1}{T}-\frac{1}{T_0}\right)\right]\varphi\, y_A \tag{5}$$

where T_0 is the average temperature used during the reaction experiments.

A classical approach while describing catalyst decay is to consider catalyst decay as function of time-on-stream. A classical relationship is the one proposed by Voorhies [15]:

$$\varphi = \exp(-\alpha t) \tag{6}$$

where α is a constant and t is the time the catalyst is exposed to a reactant atmosphere (time–on-stream).

Combining eq. (5) and eq. (6) yields:

$$\frac{-V}{W_c}\frac{dy_A}{dt} = k'_0 \exp\left[\frac{-E_R}{R}\left(\frac{1}{T}-\frac{1}{T_0}\right)\right]\exp\left(-\alpha t\right) y_A \tag{7}$$

Catalyst activity decay function can also be expressed as a function of the converted reacted, where coke formation is considered to be in proportion to the conversion of the

hydrocarbon. This approach is referred to as the Reactant Converted (RC) Model. The deactivation function is given in ref. [14] as:

$$\varphi = \exp\left[-\lambda\left(1 - y_A\right)\right] \tag{8}$$

Equation (6) in terms of RC model then becomes:

$$-\frac{V}{W_c}\frac{dy_A}{dt} = k_o' \exp\left[\frac{-E_R}{R}\left(\frac{1}{T} - \frac{1}{T_o}\right)\right]\exp\left[-\lambda\left(1 - y_A\right)\right] y_A \tag{9}$$

4. RESULTS AND DISCUSSIONS

Catalytic experiments involving three valuable model compounds (1,3,5-TIPB, 1,4-DIPB and n-dodecane) were performed in a riser simulator over two different FCC catalysts. Experiments were carried out at catalyst/reactant ratio of 5; residence times of 5,7,10 and 15 s; and temperatures of 350, 400 and 450^{o}C. During the course of the investigation, a number of runs were repeated to check for reproducibility in the conversion results, which was found to be excellent. Typical errors were in the range of ± 2%.

4.1 Activity & Selectivity of the catalysts

4.1.1 Cracking of 1,3,5-Triisopropylbenzene (1,3,5-TIPB): The conversion of 1,3,5-TIPB was studied over two different catalysts loaded in the riser simulator under various operating conditions of temperatures (350, 400 and 450^{o}C) and reaction times (5,7,10 and 15s). It is observed that for both catalysts and for all temperatures studied, conversion of 1,3,5-TIPB increases with reaction time. This is consistent with physical principles as the larger residence times offer an increased opportunity for the molecule to be cracked further. However, this trend gets moderated at larger residence times due to coke formation.

The effect of temperature on 1,3,5-TIPB is reported in Figures 3 and 4. At 15s, for the FCC-GKF catalyst (Fig. 3), the conversion increased from 13.17% at 350^{o}C to 16.05% at 400^{o}C, an increase of about 22%. However, the conversion increased tremendously from 16.05% at 400^{o}C to about 24% at 450^{o}C, an increase of about 50%. This phenomenon has also been observed in the FCC-B catalyst (Fig.4) to even a higher degree. The conversion rose from 11.23% at 350^{o}C to 18.86% at 400^{o}C and then to 27.06% at 450^{o}C, corresponding to relative increases in conversion of 67.9% and 43% respectively.

Figures 5 and 6 compare the catalytic conversions of 1,3,5-TIPB attained over the two FCC catalysts at 7 and 10s reaction times. It is apparent that at higher temperatures (400 and 450^{o}C), even though the acidity of the FCC-GKF catalyst is almost 8 times higher than that of the FCC-B, the two catalysts show comparable conversions within experimental errors. This seems to suggest that diffusion constraint molecule such as 1,3,5-TIPB with a critical diameter of 9.5Å could still evolve in the 7.4Å openings of the

FCC-B zeolite catalyst. It is also possible that 1,3,5-TIPB is pre-cracked by the wide pore matrix. And more importantly, it goes to show that weaker acid sites are sufficient for alkyl benzene cracking. This chemical event is iluustrated in Fig. 7. At lower temperature (350^oC), cracking over the FCC-GKF catalyst gives higher conversions as compared to those obtained using the FCC-B catalyst at all residence times investigated.

Analytical investigations of 1,3,5-TIPB catalytic products yielded five major products; propylene, benzene, cumene, 1,3-DIPB and some isomers of TIPB. The product distribution of 1,3,5-TIPB cracking leads to the conclusion reported in an earlier investigation [10] suggesting three step series reactions:

a) dealkylation of 1,3,5-TIPB to form 1,3-DIPB and propylene

b) dealkylation of 1,3-DIPB to give cumene and propylene

c) dealkylation of cumene to form benzene.

Besides these dominant steps, there are side reactions such as disproportionation, isomerization and condensation that may affect the gas phase product distributions and coke formation.

With regards to selectivity, FCC-GKF catalyst showed lower selectivity to cumene as compared to the FCC-B even though it has larger micro channels. But on the other hand, it has the higher selectivity for benzene. This goes to suggest that both acid properties and accessibility to the internal active sites have tremendous influence on activity and selectivity of FCC catalysts.

4.1.2 Cracking of 1,4-Diisopropylbenzene (1,4-DIPB): Cracking of 1,4-DIPB was studied under the same operating conditions as those of 1,3,5-TIPB. As expected, conversions of 1,4-DIPB were found to increase with reaction time and with increases in temperature. A summary of the results are given in Figures 8 and 9.

Conversion of 1,4-DIPB showed moderate temperature dependence at low reaction times for both the two catalysts. At 5s reaction time for the FCC-GKF (Fig. 8), the conversion increased from 11.30% at 350^oC to 13.53% at 400^oC and to only 15.18% at 450^oC. Similarly, for FCC-B, the conversion increased form 8.35% at 350^oC, to 11.26% at

400°C and to 13.02% at 450°C. At higher residence times, the temperature dependence is more pronounced.

Figures 10 and 11 compare the conversions of 1,4-DIPB attained over the two catalysts at 7 & 10s reaction times and various temperatures. At the lowest temperature of 350°C (Fig. 11), the FCC-GKF catalyst gave higher conversion than the FCC-B at all reaction times. This could be due to the higher acidity of the GKF as compared to the FCC-B despite easy accessibility of the 1,4-DIPB molecule (6.8Å) through the FCC-B catalyst as compared to the GKF's pores. At higher temperatures of 400 and 450°C (Figs. 10 and 11), it is observed that at lower reaction times, the two catalysts gave conversions of comparable values within the experimental error of ± 2%. Similar observation was also noted in relation to the 1,3,5-TIPB cracking.

The main reaction products of 1,4-DIPB reaction are gases, cumene, benzene and DIPB isomers. Some other products identified though in minor amounts include, toluene and xylenes. The product distribution seems to suggest a two step dealkylation reactions; the first being the dealkylation of 1,4-DIPB to form cumene and propylene, and then the dealkylation of the cumene to give benzene and propylene.

The selectivity of the cumene is again lower in the FCC-GKF as compared to FCC-B. But the situation is completely opposite for benzene selectivity with the FCC-GKF posting higher selectivity values. This behavior is expected and is consistent with physical principles since the production of benzene is at the expense of cumene conversion to benzene.

4.1.2 Cracking of n-Dodecane: Catalytic cracking of n-dodecane was also studied over the two catalyst at 350, 400 and 450°C temperatures and 5,7,10 & 15s reaction times. Figures 12 and 13 report the results obtained. As seen in the previous hydrocarbon molecules, in n-dodecane as well, for both catalysts and for all the temperatures investigated, n-dodecane conversion increased with reaction times. And in all the experimental runs, it was observed that the FCC-GKF catalyst posted much higher conversions for n-dodecane as compared to FCC-B, and in some instances up to 5 folds. Figures 14 and 15 compare the conversions of 1,4-DIPB attained over the two catalysts at 7 & 10s reaction times and various temperatures.

Using n-dodecane with a critical molecular diameter of 4.9Å [11], the catalytic activity is most affected by the acid properties of the catalyst because this straight chain hydrocarbon has access to the internal active sites of the materials used. Therefore, it is not surprising that FCC-GKF with acidity 8 times higher than FCC-B to have higher conversions.

4.2 Apparent Kinetic Parameters and Model Predictions

4.2.1 1,3,5-Triisopropylbenzene (1,3,5-TIPB): The apparent kinetic parameters (*ko,* E_R & α) for the TOS model and (*ko,* E_R & λ) for the RC model were determined for each of the catalyst studied using non linear regression of the experimental data of the conversions. The deactivation constant for the TOS model (α) was constrained to lie between 0.1 and 0.5 to be consistent with literature values [12,14]. Similarly, the deactivation constant for the RC model (λ) was constrained to lie between 2 and 7 [5, 14].

Table 2 reports the apparent kinetic parameters obtained for 1,3,5-TIPB catalytic conversions over the two FCC catalysts along with their corresponding 95% confidence limits for the TOS model. The correlation matrixes (Tables 3 and 4) displayed low cross-correlation between the regressed parameters showing that the kinetic parameters have been properly evaluated.

From the results of the kinetic parameters presented in Table 2, it is observed that a value of 5.39 kcal/mol was obtained as the activation energy (E_R) of 1,3,5-TIPB cracking over the FCC-GKF, while a higher value of 7.98 kcal/mol was obtained for the Y zeolite FCC-B. The ease of cracking in the FCC-GKF even though it has smaller pore size as compared to the Y zeolite can be attributed to the fact that the 1,3,5-TIPB does not fit into the pores of the FCC-GKF catalyst and thus, it has to react on the active sites on the external surface of the ZSM-5. The higher value of 7.98 kcal/mol in the FCC-B can be explained in relation to the geometrical access limitation of the 1,3,5-TIPB (9.5Å) into the FCC-B zeolite with the pore opening of 7.4Å. The pre-exponential factors give an indication of the number of active sites of the catalyst. It is therefore very consistent that FCC-GKF with higher acidity should have higher pre-exponential factor (*ko*) higher than FCC-B. The values obtained as reported in Table 2 confirm this. Values for the deactivation constant (α) have also been reported in Table 2. The higher value of 0.19 sec^{-}

[1] was obtained for the FCC-GKF as compared to a value of 0.11 sec^{-1} obtained for FCC-B in relation to 1,3,5-TIPB cracking.

Figs. 3 & 4 show comparisons between experimental conversions and model predicted values. As observed in these plots, the model predictions compare favorably with the obtained experimental data for the various conditions. As indicated in Table 2, the parameters fit to the data gives regression coefficients of 0.94 and 0.98 for FCC-GKF & FCC-B, respectively.

The values of the activation energies obtained in this study are in the same range as those found by Kraemer [12] for the cracking of alkylaromatics in the riser simulator using a time-on –stream model.

The apparent kinetic parameters obtained for 1,3,5-TIPB catalytic conversions over the two FCC catalysts along with their corresponding 95% confidence limits for the RC model are reported in Table 5 . The correlation matrixes (Tables 6 and 7) also displayed low cross-correlation between the regressed parameters. The activation energies obtained for the RC model are higher than those obtained using the TOS model. 8.69 kcal/mol was obtained as the activation energy (E_R) for 1,3,5-TIPB cracking over the FCC-GKF , while a higher value of 11.40 kcal/mol was obtained for the Y zeolite FCC-B. Similarly, FCC-GKF with higher acidity exhibits higher pre-exponential factors (*ko*) higher than FCC-B. A higher value of 7.07 was obtained for the deactivation constant (λ) for the FCC-GKF as compared to a value of 5.04 obtained for FCC-B.

4.2.2 1,4-Diisopropylbenzene (1,4-DIPB): Table 8 reports the apparent kinetic parameters (*ko,* E_R & α) obtained for 1,4-DIPB catalytic conversions over the two FCC catalysts along with their corresponding 95% confidence limits for the TOS model. The correlation matrixes (Tables 9 and 10) displayed low cross-correlation between the regressed parameters showing that the kinetic parameters are accurate.

From the results of the kinetic parameters presented in Table 5, it is observed that a value of 3.86 kcal/mol was obtained as the activation energy (E_R) of 1,4-DIPB cracking over the FCC-GKF, while a slightly higher value of 4.71 kcal/mol was obtained for the Y zeolite FCC-B. The slight ease of cracking in the FCC-GKF even though it has smaller pore size as compared to the Y zeolite can be attributed to the fact that it has higher acidity (8

times) compared to the Y-zeolite. It is worth noting that 1,4-DIPB with a critical diameter of (6.8Å) might be able to fit into the pores of the FCC-GKF catalyst if we do not view molecules as rigid bodies. Thus, the activation energies of cracking for 1,4-DIPB should be lower than those of 1,3,5-TIPB. The pre-exponential factors reported for the 1,4-DIPB cracking in Table 8 show that the FCC-GKF with higher acidity has higher pre-exponential factor than FCC-B. Consistent with the results of the 1,3,5-TIPB cracking, the FCC-GKF catalyst gave higher deactivation constant (α) of 0.12 sec^{-1} for 1,4-DIPB cracking as compared to a value of 0.11 sec^{-1} obtained for FCC-B.

Figs. 8 & 9 show comparisons between experimental conversions and model predicted values. As observed in these plots, the model predictions compare favorably with the obtained experimental data for the various conditions. As indicated in Table 8, the parameters fit to the data gives regression coefficients of 0.98 and 0.96 for FCC-GKF & FCC-B, respectively.

The apparent kinetic parameters obtained for 1,4-DIPB catalytic conversions over the two FCC catalysts along with their corresponding 95% confidence limits for the RC model are reported in Table 11 . The correlation matrixes (Tables 12 and 13) also displayed low cross-correlation between the regressed parameters. The activation energies obtained for the RC model are higher than those obtained using the TOS model. 5.73 kcal/mol was obtained as the activation energy (E_R) for 1,4-DIPB cracking over the FCC-GKF , while a higher value of 5.77 kcal/mol was obtained for the Y zeolite FCC-B. Similarly, FCC-GKF with higher acidity exhibits higher pre-exponential factors higher than FCC-B. A higher value of 4.53 was obtained for the deactivation constant (λ) for the FCC-GKF as compared to a value of 2.2 obtained for FCC-B.

4.2.3 n-Dodecane: Table 14 reports the apparent kinetic parameters (ko, E_R & α) obtained for n-dodecane catalytic conversions over the two FCC catalysts along with their corresponding 95% confidence limits for TOS model. The correlation matrixes presented in Tables 15 and 16 showed low cross-correlation between the regressed parameters indicating very good kinetic parameters.

From the results of the kinetic parameters presented in Table 14, it is seen that a value of 3.12 kcal/mol was obtained as the activation energy (E_R) of n-dodecane cracking over the FCC-GKF, while a much higher value of 11.61 kcal/mol was obtained for the Y

zeolite FCC-B. Again the ease of cracking in the FCC-GKF even though it has smaller pore size as compared to the Y zeolite can be attributed to its higher acidity as compared to FCC-B. This result suggests that a correlation can be presented between catalyst acidity and activation energy of paraffin cracking.

It is worth noting that n-dodecane with a critical diameter of (4.9Å) is able to fit into the pores of both the two catalysts without any geometrical hindrance. Therefore, the catalytic activity in n-dodecane is most affected by the acid properties of the catalyst material. Due to its very low acidity, it is not surprising that the activation energy of cracking for n-dodecane over the Y zeolite FCC-B is highest when compared to the other two alkyl benzene molecules. The pre-exponential factors reported for the n-dodecane cracking in Table 14 again show that the FCC-GKF with higher acidity has higher pre-exponential factor (*ko*) than FCC-B. Similarly, the FCC-GKF catalyst posted a higher deactivation constant (α) of 0.12 sec^{-1} for n-dodecane cracking as compared to a value of 0.11 sec^{-1} obtained for FCC-B.

Figs. 12 & 13 show comparisons between experimental conversions and model predicted values. As observed in these plots, the model predictions compare favorably with the obtained experimental data for the various conditions. As indicated in Table 14, the parameters fit to the data gives regression coefficients of 0.97 and 0.98 for FCC-GKF & FCC-B, respectively.

The apparent kinetic parameters obtained for n-Dodecane catalytic conversions over the two FCC catalysts along with their corresponding 95% confidence limits for the RC model are reported in Table 17. The correlation matrixes (Tables 18 and 19) also displayed low cross-correlation between the regressed parameters. The activation energies obtained for the RC model are higher than those obtained using the TOS model. 3.84 kcal/mol was obtained as the activation energy (E_R) for n-Dodecane cracking over the FCC-GKF , while a higher value of 14.00 kcal/mol was obtained for the Y zeolite FCC-B. Similarly, FCC-GKF with higher acidity exhibits higher pre-exponential factors higher than FCC-B. A higher value of 3.78 was obtained for the deactivation constant (λ) for the FCC-B as compared to a value of 2.11 obtained for FCC-GKF.

6. CONCLUSIONS

The catalytic cracking of three model hydrocarbons, n-dodecane and two alkyl benzenes (1,3,5-TIPB, and 1,4-DIPB) have been tested using Y and ZSM-5 zeolites. This study gives an impetus to the fact that riser simulator can be used effectively in investigating catalytic cracking reactions.

n-Dodecane with a critical diameter of 4.9Å is able to fit into the pores of both the two catalysts without any geometrical hindrance. The results of this study have shown that the activation energy of cracking for n-dodecane over the Y zeolite FCC-B (low acidity) is higher as compared to the activation energy of cracking of the same molecule over the FCC-GKF catalyst (higher acidity). Therefore, The catalytic activity in n-dodecane is most affected by the acid properties of the catalyst material. The activation energy of cracking for n-dodecane over the Y zeolite catalyst FCC-B has been found to be the highest among the three model hydrocarbons, 11.61 kcal/mol [TOS model] and 14.00 kcal/mol [RC model], indicating the necessity of stronger acid sites for n-alkanes cracking like n-dodecane. On the contrary, n-dodecane cracking over the FCC-GKF zeolite catalyst gave the lowest activation energy as compared to the alkyl benzenes.

At higher temperatures (400 and 450^{o}C), even though the acidity of the FCC-GKF catalyst is almost 8 times higher than that of the FCC-B, the two catalysts show comparable conversions for 1,3,5-TIPB and 1,4-DIPB at all reaction times (within experimental errors). This goes to show that weaker acid sites may be sufficient for alkyl benzene cracking and the internal active sites of the FCC-GKF were not used effectively due to diffusion limitation.

Acknowledgement

The authors gratefully acknowledge King Fahd University of Petroleum & Minerals for the financial support for this work under Project ARI-029.

Nomenclature

C_A	reactant concentration in the riser simulator (mole/m^3)
CFL	confidence limit
E_R	energy of activation energy, kcal/mol
k	apparent kinetic rate constant (m^3/kgcat.sec). $= k'_0 \exp[\frac{-E_R}{R}(\frac{1}{T}-\frac{1}{T_0})$
$k_o^{'}$	Pre-exponential factor in Arrhenius equation defined at an average temperature [m^3/kgcat.sec], units based on first order reaction
MW_A	molecular weight of specie A
r	correlation coefficient
R	universal gas constant, kcal/kmol K
t	reaction time (sec).
T	reaction temperature, K
To	average temperature of the experiment, 673 K
V	volume of the riser (45 cm^3)
W_c	mass of the catalysts (0.81 gcat)
W_{hc}	total mass of hydrocarbons injected in the riser (0.162 g)
y_A	reactant mass fraction (wt%)

Greek letters

α	apparent deactivation constant, s^{-1} (TOS Model)
λ	apparent deactivation constant, (RC Model)
φ	apparent deactivation function, dimensionless

Literature Cited

1. Corma, A., Melo, F. V., Sauvanaud, L, and Ortega, F. J. "*Different process schemes for converting light straight run and fluid catalytic cracking naphthas in a FCC unit for maximum propylene production*", Appl. Catal., A: General 265(2) (2004) 195-206.

2. Al-Khattaf, S, and de Lasa, H. "*The role of diffusion in alkyl benzenes catalytic cracking*", Appl. Catal., A: general 226 (2002) 139-153.

3. Humphries, A., and Wilcox, J. "*Zeolite components and matrix composition determine FCC catalyst performance*", Oil & Gas J., Feb., 6 (1989) 45-51.

4. Krager, J., and Ruthven, D. M., "*Diffusion in Zeolites and other Microporous Solids",* Wiley, New York, 1992.

5. Al-Khattaf, S, Atias, J. A., Jarosch, K., and de Lasa, H. "*Diffusionand catalytic cracking of 1,3,5 tri-iso-propyl-benzene in FCC catalysts*", Chem. Eng. Sci., 57 (2002) 4909-4920.

6. Roos, K., Liepoid, A., Koch, H., and Reschetilowski, W. "*Impact of accessibility and activity on novel molecular sieves for catalytic cracking of hydrocarbons*" Chem. Eng . Technol. 20 (1997) 326-332.

7. Abbot, J., and Wojciechowski, B. W. "*Catalytic Reactions of n-Dodecane on Aluminosilicates*" J. of Catalysis, 115 (1989) 521-531.

8. Corma, A., Miguel, P. J., and Orchilles, A. V. "*Kinetics of the Catalytic Cracking of Paraffins at Very Short Times on Stream*" J. of Catalysis, 145 (1994) 58-64.

9. de Lasa, H. T., US Patent 5 (102) (1992) 628.

10. Al-Khattaf, S., "*The Influence of Y-zeolite Unit cell Size on the Performance of FCC Catalyst during Gas oil Catalytic Cracking*" Appl. Catal. A: 231 (2002) 293.

11. Al-Khattaf, S, and de Lasa, H. I. "*Diffusion and Reactivity of Hydrocarbon Feedstocks in FCC Catalyst"* Can. J. Chem. Eng. 79 (2001) 329.

12. Kraemer, D. W., Ph.D. Dissertation, University of Western Ont., London, Canada 1991.

13. Corma, A., and B. W. Wojciechowski, "*The Catalytic Cracking of Cumene*" Catal. Rev. Sci. Eng. 24 (1) (1982) 1-65.

14. Al-Khattaf, S, and de Lasa, H. I. "*Catalytic Cracking of Cumene in a Riser Simulator: A Catalyst Activity Decay Model"* Ind. Eng. Chem. Res. 40 (2001) 5398.

15. Voorhies, A. Jr., Ind. Eng. Chem., 37 (1945) 318.

List of Tables

Table 1: Properties of the Catalyst used in this study

	Y-zeolite (FCC-B)	ZSM-5 (FCC-GKF)
BET surface area (m^2/g)	155	69
Acidity (mmol/g)	0.033	0.233
Na_2O (wt %)	negligible	negligible

Table 2: Kinetic constants for both FCC-GKF and FCC-B (for 1,3,5-TIPB) Based on Time on Stream (TOS Model)

Catalyst	k_0 (m^3/kg-cat.sec)	95% CFL	E_R (kcal/mol)	95% CFL	α (1/sec)	95% CFL	r^2
FCC-GKF	2.31E-03	0.51E-03	5.39	1.25	0.19	0.06	0.94
FCC-B	1.59E-03	0.26E-03	7.98	1.14	0.11	0.04	0.98

Table 3: Correlation matrix for FCC-GKF (1,3,5-TIPB) – TOS Model

k_0	1	-0.10	0.97
E_R	-0.10	1	-0.01
α	0.97	-0.01	1

Table 4: Correlation matrix for FCC-B (1,3,5-TIPB) – TOS Model

k_0	1	-0.18	0.95
E_R	-0.18	1	-0.02
α	0.95	-0.02	1

Table 5: Kinetic constants for both FCC-GKF and FCC-B (for 1,3,5-TIPB) Based on Reactant Conversion (RC Model)

Catalyst	k_0 (m^3/kg-cat.sec)	95% CFL	E_R (kcal/mol)	95% CFL	λ	95% CFL	r^2
FCC-GKF	1.97E-03	1.19E-03	8.69	4.58	7.07	6.08	0.88
FCC-B	1.51E-03	0.38E-03	11.40	2.49	5.04	2.63	0.98

Table 6: Correlation matrix for FCC-GKF (1,3,5-TIPB) – RC Model

k_0	1	0.60	0.98
E_R	0.60	1	0.65
λ	0.98	0.65	1

Table 7: Correlation matrix for FCC-B (1,3,5-TIPB) – RC Model

k_0	1	0.60	0.95
E_R	0.60	1	0.71
λ	0.95	0.71	1

Table 8: Kinetic constants for both FCC-GKF and FCC-B (for 1,4-DIPB) Based on Time on Stream (TOS Model)

Catalyst	k_0 (m^3/kg-cat.sec)	95% CFL	E_R (kcal/mol)	95% CFL	α (1/sec)	95% CFL	r^2
FCC-GKF	2.26E-03	0.29E-03	3.86	0.82	0.12	0.03	0.98
FCC-B	2.20E-03	0.76E-03	4.71	2.23	0.11	0.08	0.96

Table 9: Correlation matrix for FCC-GKF (1,4-DIPB) – TOS Model

k_0	1	-0.08	0.96
E_R	-0.08	1	-0.02
α	0.96	-0.02	1

Table 10: Correlation matrix for FCC-B (1,4-DIPB) – TOS Model

k_0	1	-0.10	0.96
E_R	-0.10	1	-0.02
α	0.96	-0.02	1

Table 11: Kinetic constants for both FCC-GKF and FCC-B (for 1,4-DIPB) Based on Reactant Conversion (RC Model)

Catalyst	k_0 (m^3/kg-cat.sec)	95% CFL	E_R (kcal/mol)	95% CFL	λ	95% CFL	r^2
FCC-GKF	2.36E-03	0.58E-03	5.73	1.64	4.53	1.95	0.97
FCC-B	1.69E-03	0.27E-03	5.77	1.22	2.2	1.30	0.99

Table 12: Correlation matrix for FCC-GKF (1,4-DIPB) – RC Model

k_0	1	0.47	0.97
E_R	0.47	1	0.51
λ	0.97	0.51	1

Table 13: Correlation matrix for FCC-B (1,4-DIPB) – RC Model

k_0	1	0.44	0.96
E_R	0.44	1	0.52
λ	0.96	0.52	1

Table 14: Kinetic constants for both FCC-GKF and FCC-B (for n-DODECANE) Based on Time on Stream (TOS Model)

Catalyst	k_0 (m^3/kg-cat.sec)	95% CFL	E_R (kcal/mol)	95% CFL	α (1/sec)	95% CFL	r^2
FCC-GKF	2.34E-03	0.80E-03	3.12	2.15	0.12	0.08	0.97
FCC-B	0.64E-03	0.07E-03	11.61	2.37	0.11	0.06	0.98

Table 15: Correlation matrix for FCC-GKF (n-DODECANE) – TOS Model

k_0	1	-0.06	0.96
E_R	-0.06	1	-0.01
α	0.96	-0.01	1

Table 16: Correlation matrix for FCC-B (n-DODECANE) – TOS Model

k_0	1	-0.28	0.93
E_R	-0.28	1	-0.01
α	0.93	-0.01	1

Table 17: Kinetic constants for both FCC-GKF and FCC-B (for n-DODECANE) Based on Reactant Conversion (RC Model)

Catalyst	k_0 (m^3/kg-cat.sec)	95% CFL	E_R (kcal/mol)	95% CFL	λ	95% CFL	r^2
FCC-GKF	1.83E-03	0.25E-03	3.84	0.91	2.11	1.05	0.99
FCC-B	0.44E-03	0.06E-03	14.0	1.96	3.78	2.88	0.99

Table 18: Correlation matrix for FCC-GKF (n-DODECANE) – RC Model

k_0	1	0.34	0.96
E_R	0.34	1	0.39
λ	0.96	0.39	1

Table 19: Correlation matrix for FCC-B (n-DODECANE) – RC Model

k_0	1	0.36	0.87
E_R	0.36	1	0.69
λ	0.87	0.69	1

Figure Captions

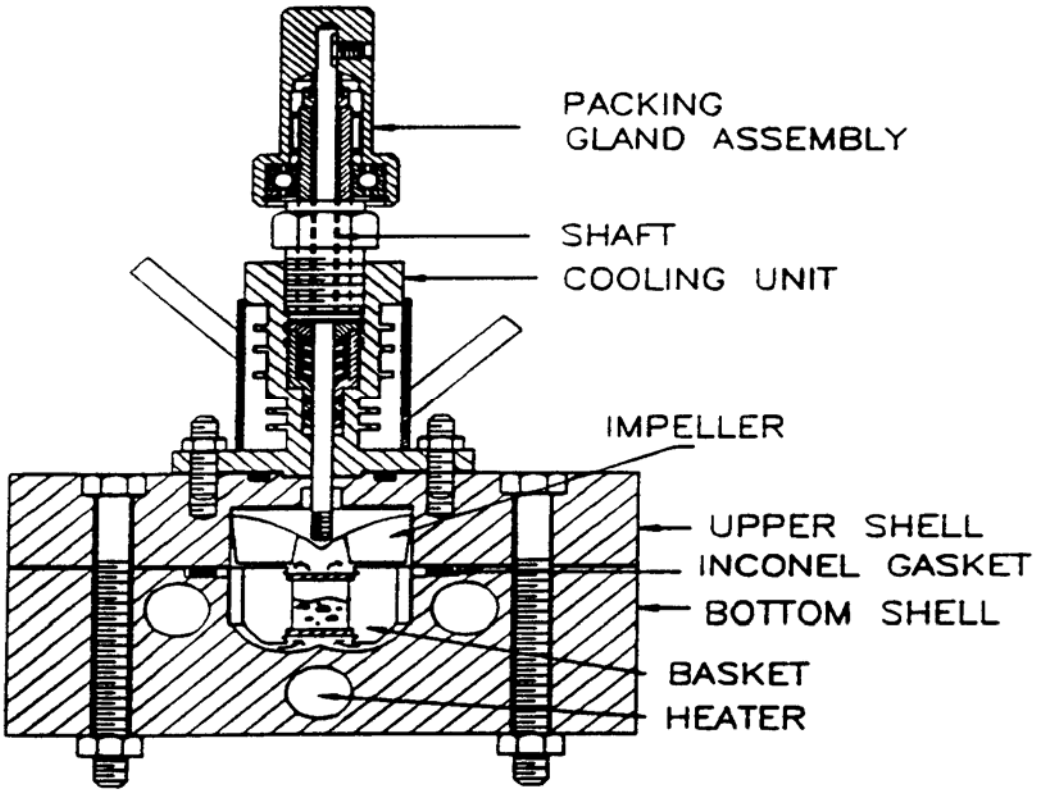

Figure 1: Schematic Diagram of the Riser Simulator

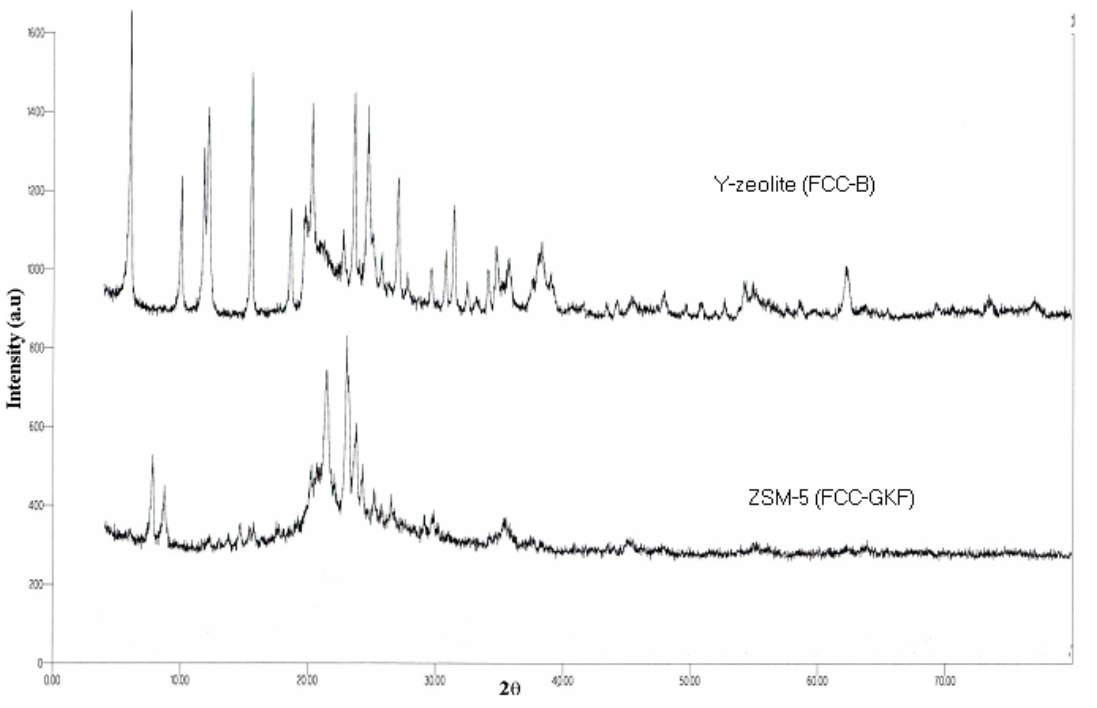

Figure 2: X-ray Diffraction for the catalysts used in the study

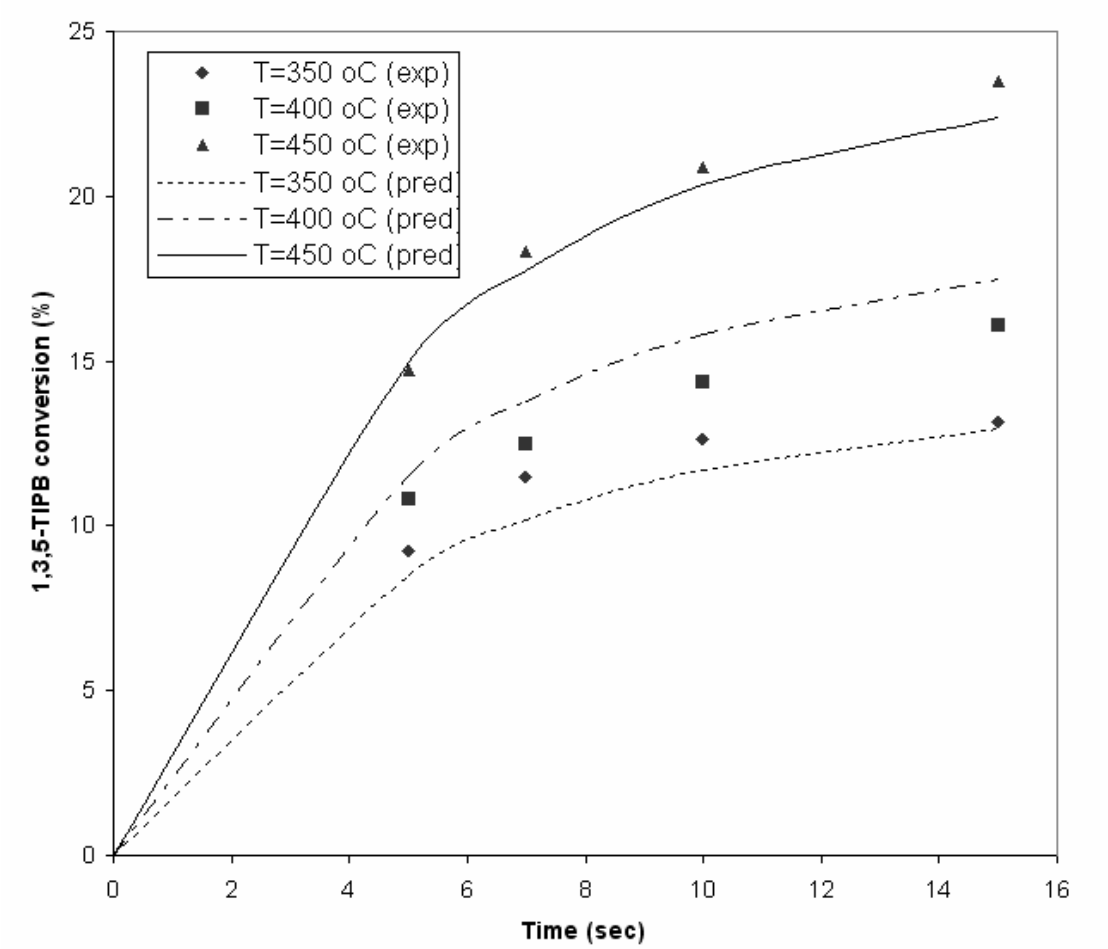

Figure 3: Modeling 1,3,5-TIPB conversion (FCC-GKF). Decay function based on time on stream (TOS)

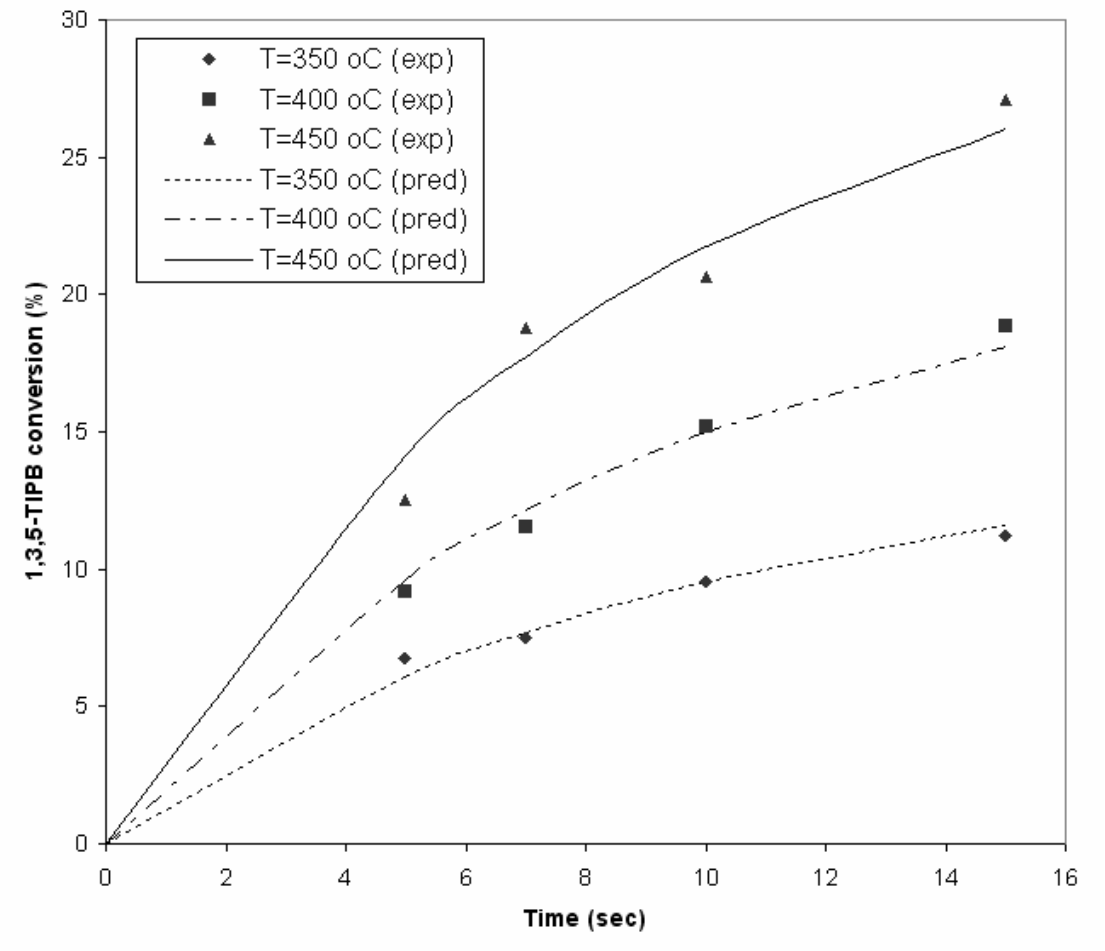

Figure 4: Modeling 1,3,5-TIPB conversion (FCC-B). Decay function based on time on stream (TOS)

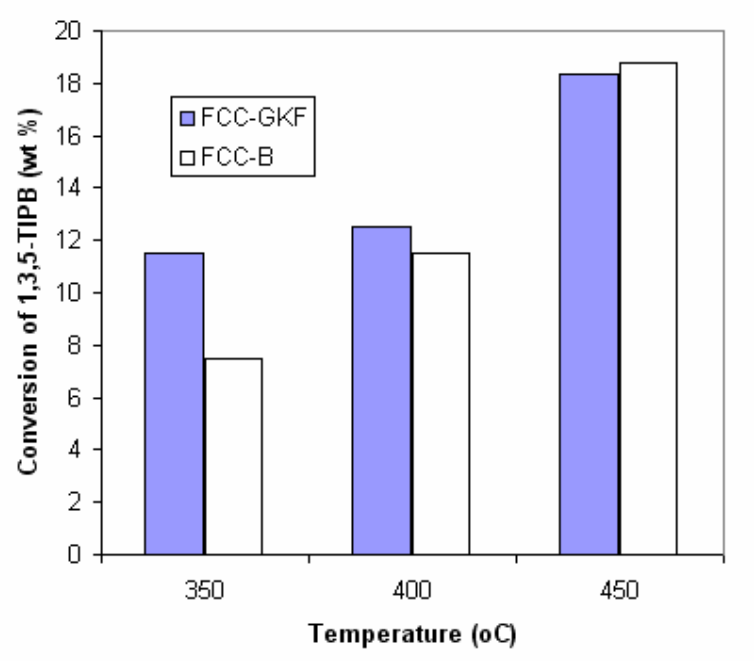

Figure 5: 1,3,5-TIPB conversion at 7-s reaction time and various temperatures

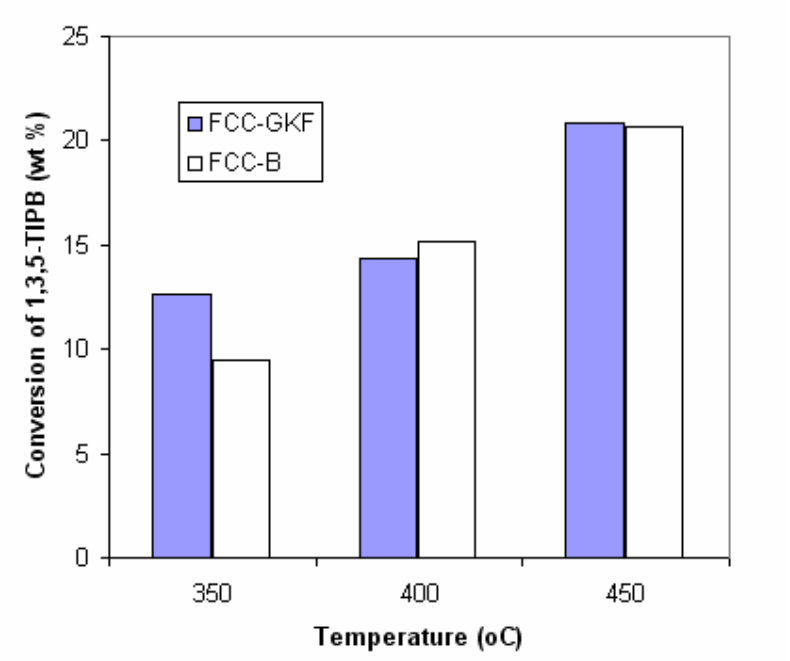

Figure 6: 1,3,5-TIPB conversion at 10-s reaction time and various temperatures

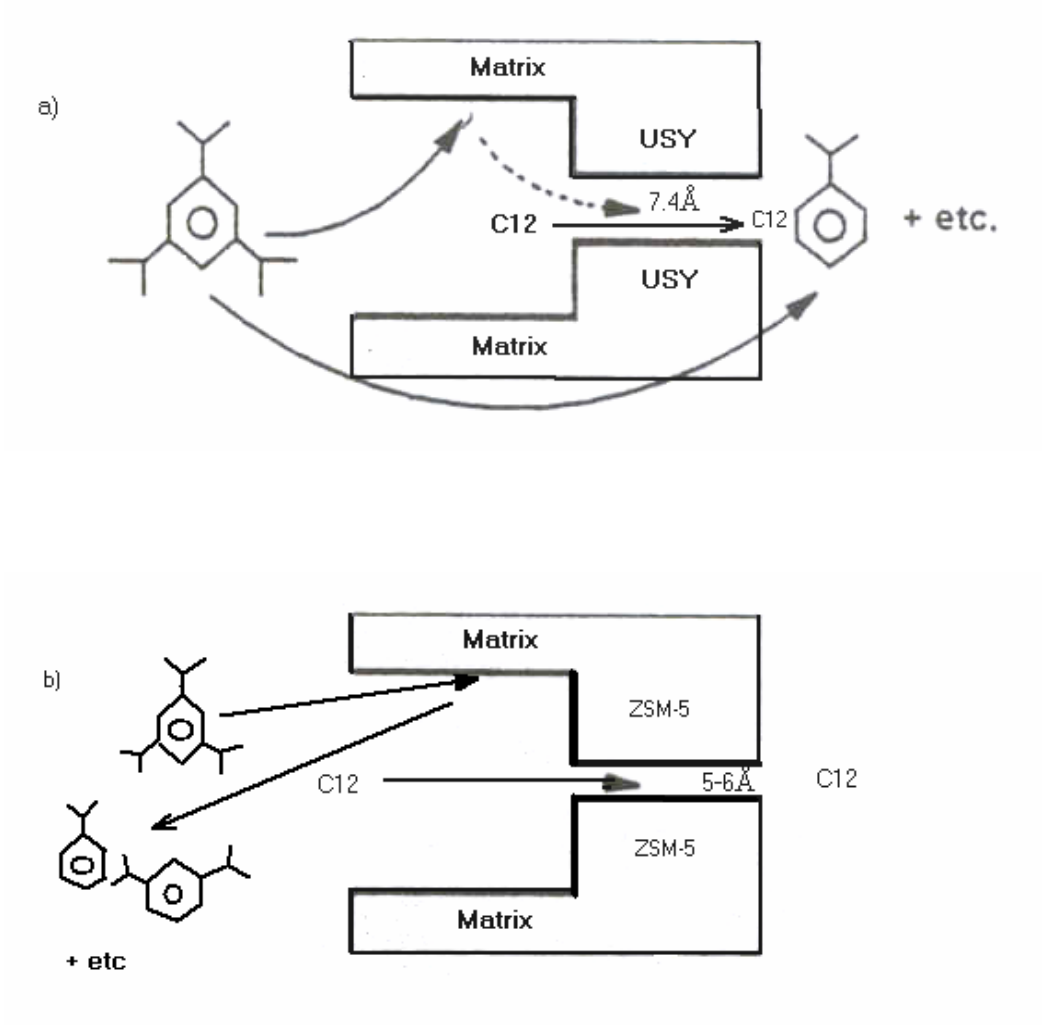

Figure 7: Effect of Pore Accessibility for 1,3,5-TIPB and n-dodecane cracking

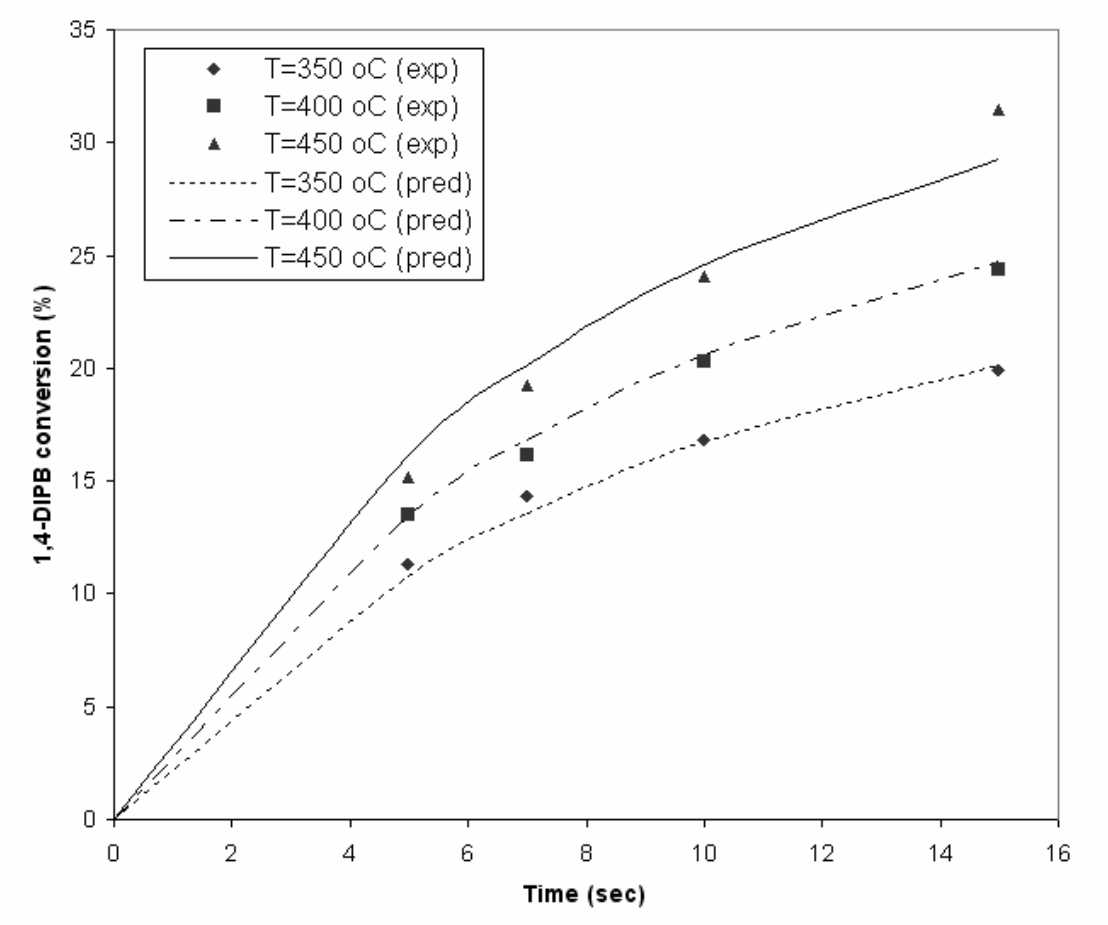

Figure 8: Modeling 1,4-DIPB conversion (FCC-GKF). Decay function based on time on stream (TOS)

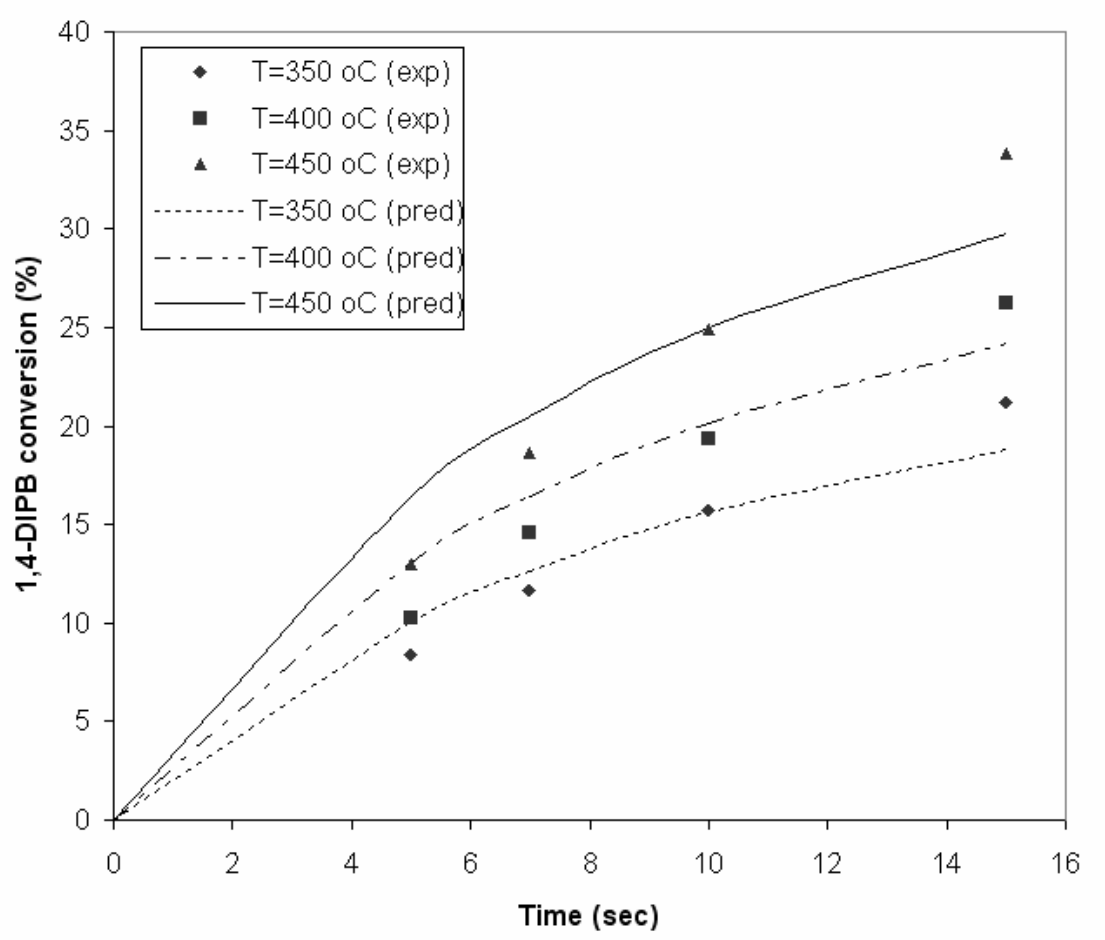

Figure 9: Modeling 1,4-DIPB conversion (FCC-B). Decay function based on time on stream (TOS)

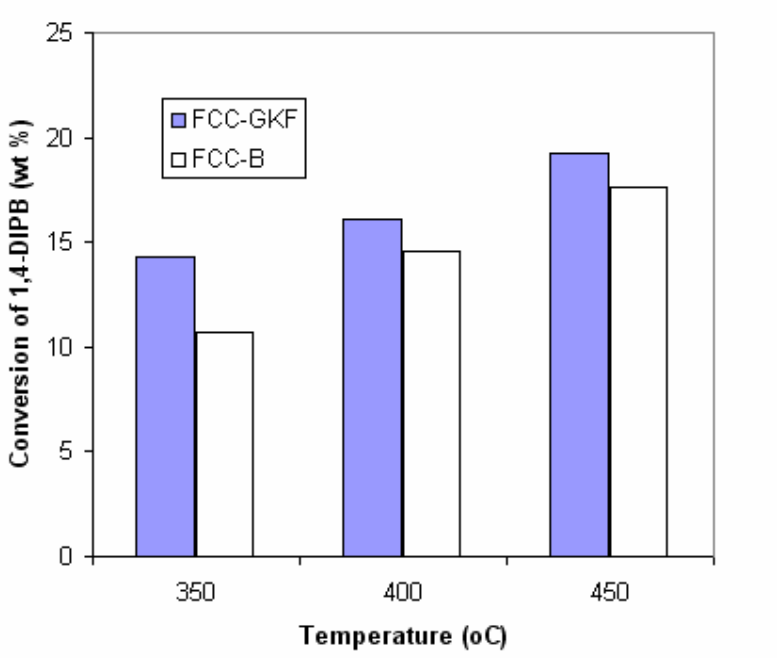

Figure 10: 1,4-DIPB conversion at 7-s reaction time and various temperatures

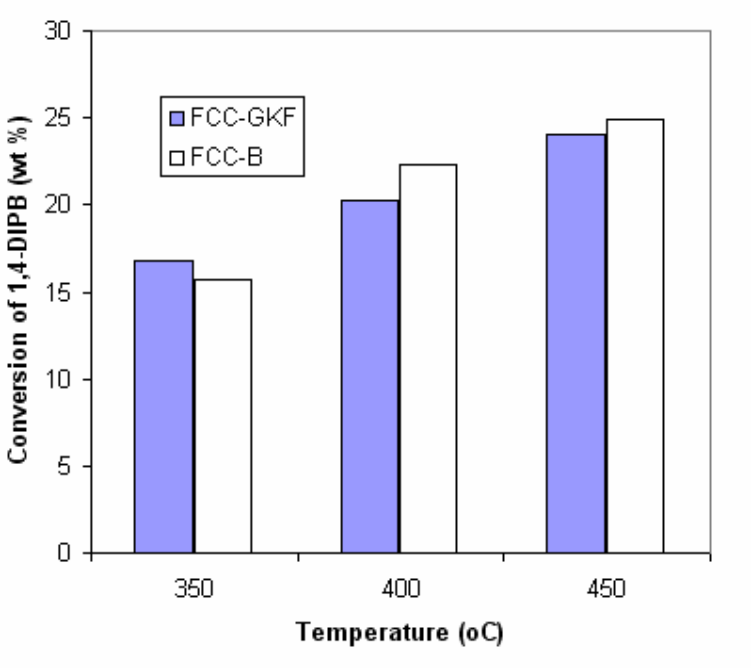

Figure 11: 1,4-DIPB conversion at 10-s reaction time and various temperatures

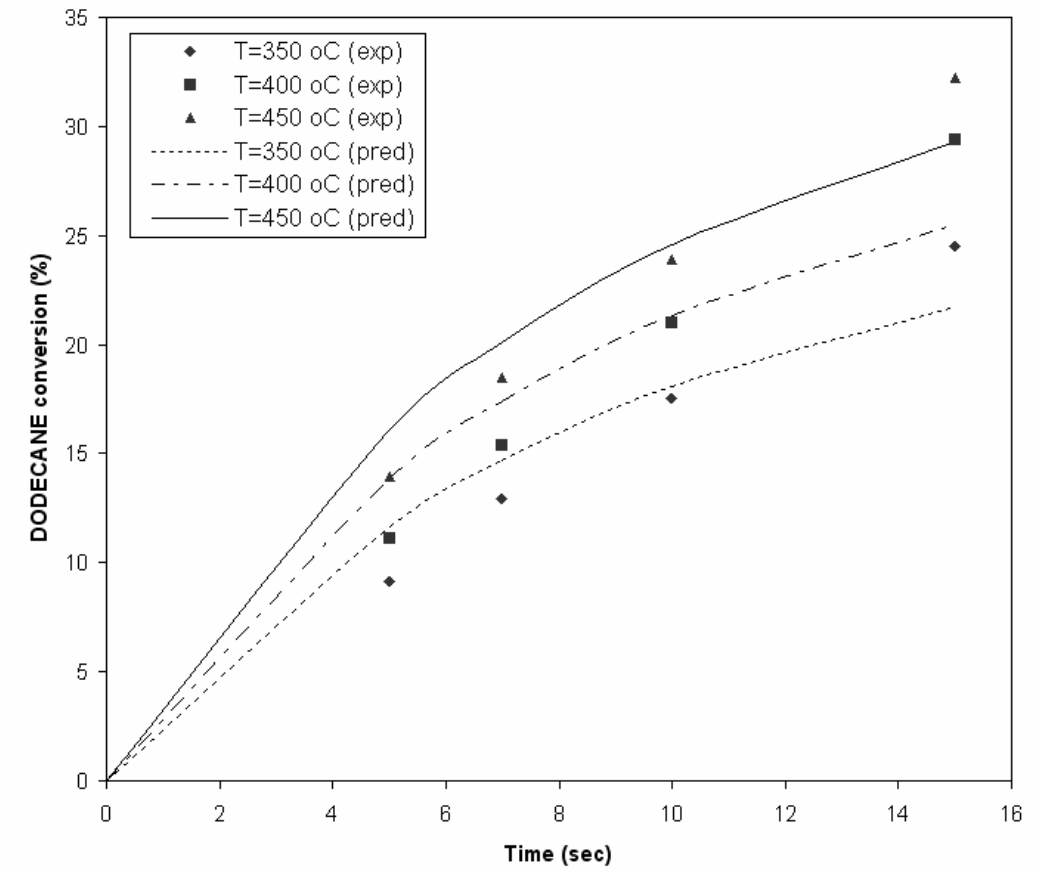

Figure 12: Modeling DODECANE conversion (FCC-GKF). Decay function based on time on stream (TOS)

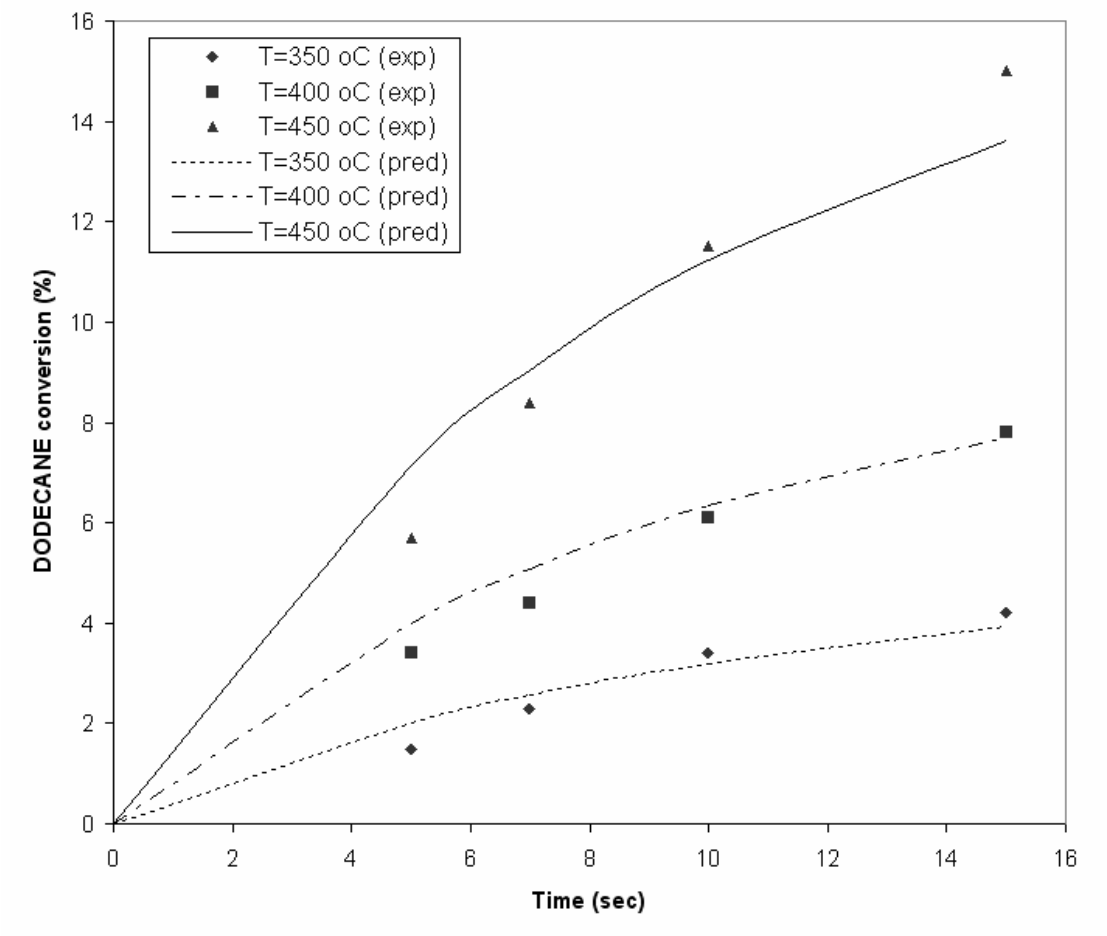

Figure 13: Modeling DODECANE conversion (FCC-B). Decay function based on time on stream (TOS)

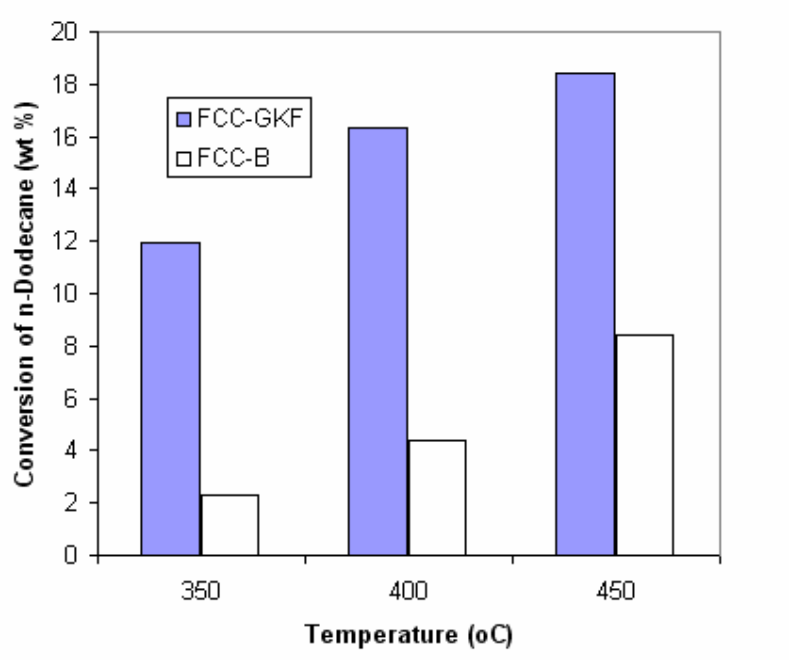

Figure 14: Dodecane conversion at 7-s reaction time and various temperatures

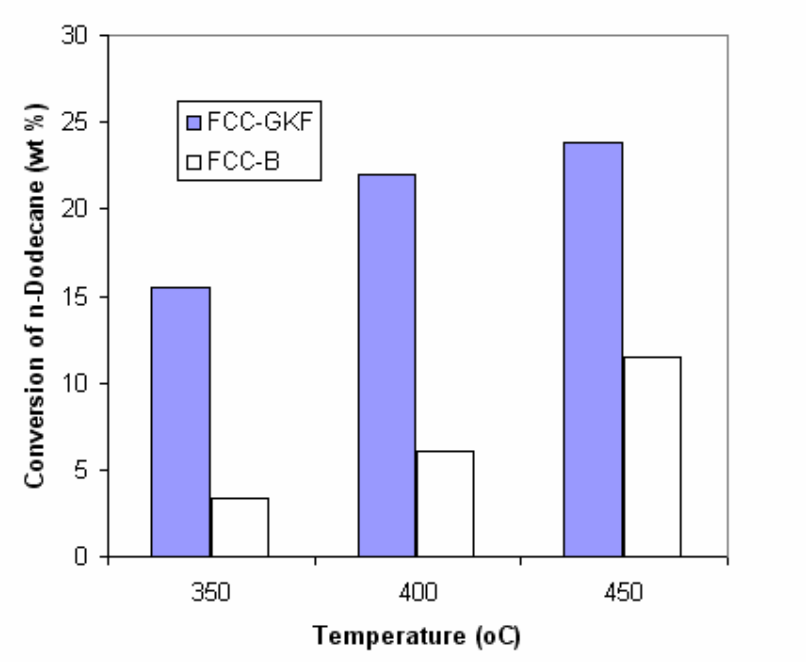

Figure 15: Dodecane conversion at 10-s reaction time and various temperatures